

Impact of Furan Substitution on the Optoelectronic Properties of Biphenyl/Thiophene Derivatives for Light Emitting Transistors

Periyasamy Angamuthu Praveen,^{*,†} Perumal Muthuraja,[‡] Purushothaman
Gopinath,[‡] and Thangavel Kanagasekaran^{*,†}

[†]*Organic Optoelectronics Research Laboratory, Department of Physics, Indian Institute of
Science Education and Research (IISER), Tirupati - 517 507, Andhra Pradesh, India*

[‡]*Department of Chemistry, Indian Institute of Science Education and Research (IISER),
Tirupati - 517 507, Andhra Pradesh, India*

E-mail: praveen@iisertirupati.ac.in; kanagasekaran@iisertirupati.ac.in

Phone: +91-877-250-0941

Abstract

Biphenyl/thiophene systems are known for their ambipolar behavior and good optical emissivity. But often these systems alone are not enough to fabricate a commercial grade light emitting devices. Especially our recent experimental and theoretical analyses on the three ring constituting thiophenes end-capped with biphenyl have shown good electrical properties but lack of good optical properties. From materials science perspective, one way to improve the properties is to modify their structure and integrate it with additional moieties. In the recent past, furan moieties are proven as the potential substitution for thiophene to improve the organic semiconductive materials

properties. In the present work, we have systematically substituted different proportion of furan rings in biphenyl/thiophene core and studied their optoelectronic properties, aiming towards organic light emitting transistor applications. We have found that the molecular planarity plays a vital role on the optoelectronic properties of the system. The lower electronegativity of the O atom offers better optical properties in the furan substituted systems. Further, the furan substitution significantly affects the molecular planarity, which in turn affects the system mobility. Due to this we have observed drastic changes in optoelectronic properties of two furan substituted systems. Interestingly, addition of furan has reduced the electron mobility by one fold than the pristine thiophene based derivative. Such a variation is interpreted to the low average electronic coupling in furan systems. Overall, systems with all furan and one ring of furan in the center, end-capped with thiophene has shown better optoelectronic properties. This molecular architecture favours more planarity in the system with good electrical properties and the transition dipole moments, both would play vital role in the construction of an organic light emitting transistor.

1 Introduction

Organic π - conjugated semiconducting systems are of great interest due to their tunable charge transfer property, that can be utilized in the technologically important areas such as organic photovoltaics (OPV), organic light emitting diodes (OLED) and organic field effect transistors (OFET), and sensors.¹⁻³ Even though, these carbon based systems are suffering of low durability than their inorganic counter parts, their tunable structure-property nature along with the flexibility, cost effectiveness and ease of fabrication made these materials as the ideal candidates for future technological endeavors. In fact, successful commercialization of OLEDs indicate the potentiality of research works in the related regimes.⁴⁻⁶

From structural point of view, rigid planar molecules such as acenes are often considered for the semiconducting devices due to their excellent charge carrier transport and mobility.

This is due to the fact that the rigidity and planarity gives rise of close crystal packing and thus reduces the reorganization energy and improves the charge transfer integrals.⁷⁻⁹ On the other hand, such a closed packing leads to strong aggregation of transition dipole moments (TDM) in the system, results photoluminescence quenching. So, better electrical or optical properties of an organic system is often the tradeoff between one another.¹⁰⁻¹³ But considering the devices like organic light emitting transistors (OLET) or long sought organic lasers, both high electrical and optical properties are required. So, often systems with high mobility and good PLQY are considered for such requirements.^{14,15}

Thiophene/phenylene derivatives are one of such systems with good mobility and high photoluminescence yield. Especially, due to its synthetic flexibility and strong polarizability, thiophene is in center of attraction for the development of optoelectronic devices over a decade.^{16,17} Presence of sulfur atoms in the thiophene's core gives rise of strong intermolecular interaction and yields excellent charge carrier mobility. Due to this, large number of reports available on these derivatives for multitude of applications ranging from OFETs to OPVs.¹⁸⁻²⁰

Our group in the past few years have reported the experimental and theoretical analysis of these thiophene/phenylene based derivatives towards OLET applications.²¹⁻²³ Our recent theoretical analysis indicates that two derivatives, 5,5''-bis(4-biphenyl)-2,2':5',2''-terthiophene (BP3T) and 2,5-bis(4-biphenyl) tetrathiophene (BP4T) shown potential optoelectronic properties.²⁴ On which BP3T has excellent electronic properties whereas BP4T has good emissive properties. Our current research interest focus on these two systems and in particular to improve the optical properties in the case of BP3T.

In this regard, we are reporting the furan substituted BP3T in the context of active medium for OLET device.²⁵ Furan is an analogues structure of thiophene, but with different physical and chemical properties. Due to their large electronegativity and weak intermolecular interactions these moieties are believed to be not suitable for the organic electronic applications for long time. But recent reports overthrow such misconceptions and indicates

the excellent charge transporting behavior in furan systems.^{26,27} Introduction of furan in a π conjugate would results small torsional angles due to the small atomic size of the oxygen. Such a reduction would improve the molecular planarity, crystal packing and overall charge transport in the system. Further, due to the size of the oxygen atom, furan does not suffers of heavy atom effect, an effect usually observed in thiophene based luminescent systems.²⁸ So, furans are expected to yield high photoluminescence yield than their structural counterpart thiophene.

Based on these facts, in the present work, we have substituted different proportions of furan in BP3T system in the place of thiophene, and studied their structural, electronic and optical properties. Since, charge transfer in the system heavily relies on the molecular planarity and rigidity, we particularly emphasized on these two properties and correlate them to the system’s optoelectronic property.

2 Methodology

General molecular structure (BPFT) of the systems that are studied in this work is given in Fig. 1. The furans are substituted from the left to right fashion, replacing thiophenes on each modification. Two special cases, where center ring accompanied by their counterparts on the either side. Each obtained geometry along with their IUPAC name is given in Table. 1 These geometries were optimized using density functional theory (DFT) calculation. B3LYP functional with 6-311G(d,p) basis set was used for the calculations.

After the geometry optimization, the nature of the stationary points were evaluated using vibrational frequencies. In the case of ionic states, spin-unrestricted formalism and time dependent DFT for excited states have been used. For the simulation of charge transfer properties we have used the hopping model. According to Einstein’s relation, mobility of an organic semiconductor at a particular temperature can be estimated by,²⁹

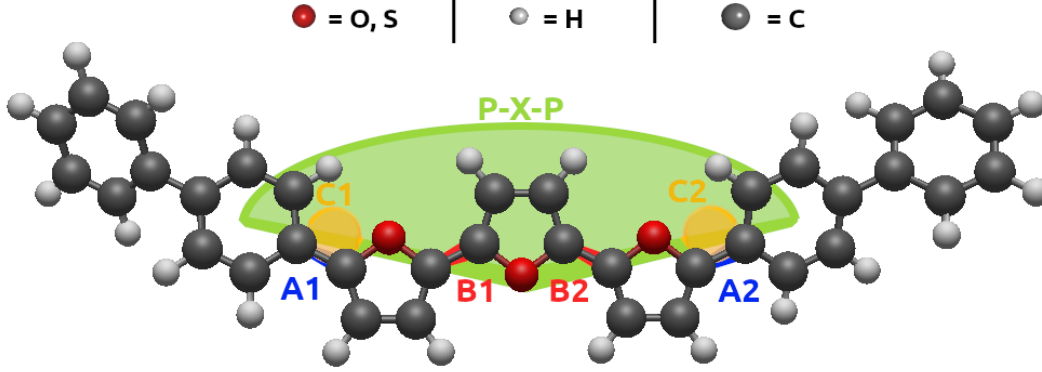


Figure 1: Molecular structure of BPFT system: A1, A2 are bond length between the phenylene and thiophene/furan rings. B1 and B2 are bond lengths between thiophene/furan rings. C1 and C2 are the bond angle between the phenylene and thiophene/furan rings. P-X-P is the dihedral angle with respect to the central ring.

$$\mu = \frac{e}{k_B T} D \quad (1)$$

here, μ is the mobility of the organic semiconductor, e is the electronic charge, k_B is the Boltzmann constant, T is the temperature and D is the diffusion coefficient given by

$$D = \frac{1}{2n} \sum_i r_i^2 W_i P_i \quad (2)$$

here P_i is the hopping probability and r_i is the hopping distance.

For the i^{th} specific hopping pathway P_i can be written as

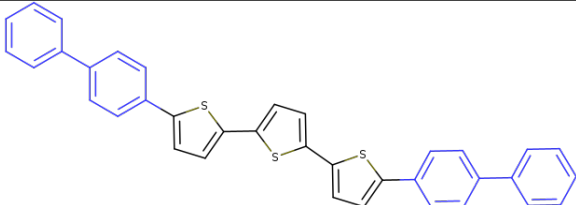
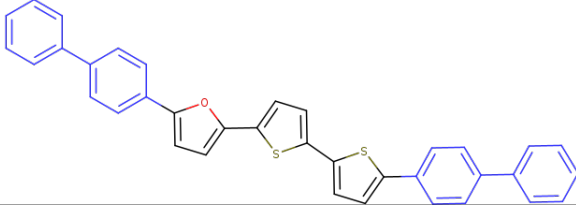
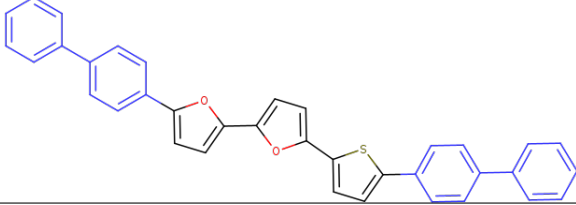
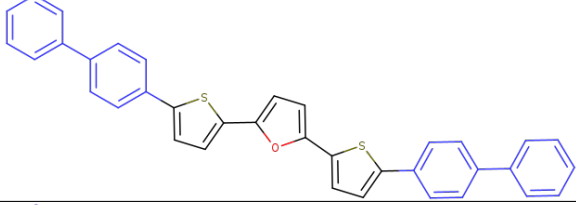
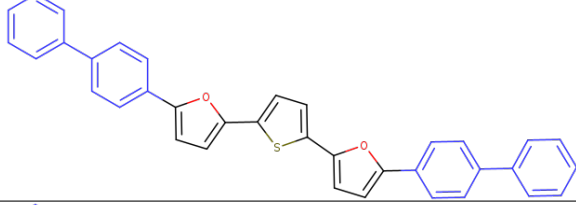
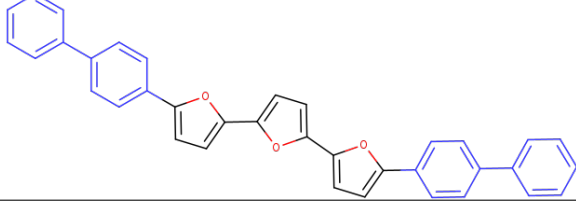
$$P_i = \frac{W_i}{\sum_i W_i} \quad (3)$$

where W equals to

$$W = \frac{V^2}{\hbar} \left(\frac{\pi}{\lambda k_B T} \right)^{1/2} \exp\left(-\frac{\lambda}{4k_B T}\right) \quad (4)$$

By solving the above Marcus-Hush equation, the non-adiabatic electronic hopping rate

Table 1: List of molecular systems used in the study and their IUPAC names

Molecule	IUPAC name	Abbreviated as
	5-{[1,1'-biphenyl]-4-yl}-5'-(5-{[1,1'-biphenyl]-4-yl}thiophen-2-yl)-2,2'-bithiophene	BP3T
	2-{[1,1'-biphenyl]-4-yl}-5-(5'-(5-{[1,1'-biphenyl]-4-yl}-[2,2'-bithiophen]-5-yl)furan	BPFTT
	5-{[1,1'-biphenyl]-4-yl}-5'-(5-{[1,1'-biphenyl]-4-yl}thiophen-2-yl)-2,2'-bifuran	BPFFT
	2,5-bis(5-{[1,1'-biphenyl]-4-yl}thiophen-2-yl)furan	BPFTF
	2-{[1,1'-biphenyl]-4-yl}-5-[5-(5-{[1,1'-biphenyl]-4-yl}furan-2-yl)thiophen-2-yl]furan	BPTFT
	5-{[1,1'-biphenyl]-4-yl}-5'-(5-{[1,1'-biphenyl]-4-yl}furan-2-yl)-2,2'-bifuran	BP3F

(W) can be estimated. Here, V is the electronic coupling between the neighboring molecules and λ is the reorganization energy of the organic semiconductor. Since, the intermolecular reorganization energies of the organic system is negligible, in the present case we have considered only the intramolecular reorganization energy and it was calculated from:

$$\lambda_{hole} = \lambda_0 + \lambda_+ = (E_0^*(Q_+) - E_0(Q_0)) + (E_+^*(Q_0) - E_+(Q_+)) \quad (5)$$

$$\lambda_{electron} = \lambda_0 + \lambda_- = (E_0^*(Q_-) - E_0(Q_0)) + (E_-^*(Q_0) - E_-(Q_-)) \quad (6)$$

where E_0 and E_+^*/E_-^* are the energies of the neutral and cationic/anionic monomer in the optimized neutral geometry Q_0 and E_0^* , and E_+/E_- are the energies of neutral and cationic/anionic monomers in the optimized cationic/anionic geometry Q_+/Q_- .

To calculate the intermolecular electronic coupling V we have used the relation,

$$V_{ij} = \left| \frac{(J_{ij} - 0.5(e_i + e_j) \cdot S_{ij})}{(1 - S_{ij}^2)} \right| \quad (7)$$

where S_{ij} is the spatial overlap, J_{ij} is the charge transfer integral and e_i and e_j are the site energies of the donor and acceptor states, respectively. These values are calculated using the relation

$$e_{i(j)} = \langle \Psi_{i(j)} | H | Psi_{i(j)} \rangle \quad (8)$$

$$S_{ij} = \langle \Psi_i | Psi_j \rangle \quad (9)$$

$$J_{ij} = \langle \Psi_i | H | Psi_j \rangle \quad (10)$$

The quantities such as the Kohn-Sham Hamiltonian of the dimer H , and $\Psi_{i(j)}$ of hole/electron transport in the monomer, were calculated using CATNIP program.^{30,31}

3 Results and Discussion

Calculated geometric parameters of furan/thiophene substituted derivatives are given in Table. 2. BPTFT retains its planar backbone from BP3T and for all other systems, the values varies with respect to the level of furan substitution in the system. When two are more number of furan rings present in the system, it influences the molecular dihedral angle. Both

BP3F and BPFTF shows the angles about 117 degrees. Interestingly, the dihedral angles of BPFFT and BPFTT are exactly same about 120.96 degrees. Calculated bond lengths, bond distances and the bond length alteration (BLA) values are given in the supplementary (Section 1). It can be seen that, with the increment in the number of furan rings BLA values decreased from 0.08 to 0.03 and BP3F shows the lowest values, indicates the highest π conjugation in the system. Also, the cationic and anionic forms of the system has lower BLA values than their neutral forms indicating the charged systems have more efficient conjugation than the neutral ones.

Table 2: Calculated geometrical parameters of BPFT system. A1, A2 are bond length between the phenylene and thiophene/furan rings. B1 and B2 are bond lengths between thiophene/furan rings. C1 and C2 are the bond angle between the phenylene and thiophene/furan rings. P-X-P is the dihedral angle with respect to the central ring. $\langle \cos^2\phi \rangle$ is the degree of backbone twisting

System	A1=A2	B1=B2	C1=C2	P-X-P	$\langle \cos^2\phi \rangle$
BP3T	1.464	1.443	120.50	159.00	0.136
BPFTT	1.451	1.431	120.96	159.03	0.137
BPTFT	1.463	1.437	121.43	173.62	0.453
BPFFT	1.451	1.431	120.96	159.03	0.137
BPFTF	1.453	1.437	117.29	138.26	0.999
BP3F	1.453	1.432	117.31	164.24	0.408

In order to explicitly extract the molecular planarity, we have measured the bond angles and bond lengths between phenyl rings and the center molecules (independent of whether furan or thiophene). In which, BPTFT shows the maximum planarity followed by BP3F, BPFTT and BPFFT, respectively. In the case of dihedral angles, upto 0.72 degrees variation has been observed (Table. 2). BPFTT and BPFFT shows the maximum and the BP3F shows the minimum ϕ value, indicates the decrement of planarity in BP3F system. A similar trend is observed in the case of anionic and cationic form of the system. But the only variation observed is that anionic form is more planar than that of the cationic form.

Since the planarity and the backbone twisting of the system is the crucial requirement to understand the functionality of the system, we have calculated the degree of backbone

twisting by estimating the $\langle \cos^2\phi \rangle$ values.³² This value is a better predictor of backbone twisting than the usual lowest-energy dihedral angles, due to the fact that the twisted molecule could be statistically more planar than the optimized state. The value can be calculated using the equation

$$\langle \cos^2\phi \rangle = \int_0^{2\pi} P(\pi) \cos^2\phi \, d\phi / \int_0^{2\pi} P(\pi) \, d\phi \quad (11)$$

where, $\langle \cos^2\phi \rangle$ is an empirical parameter to represent the planarity and orbital overlap, $P(\pi)$ is the probability distribution calculated from the Boltzmann equation and the ϕ ranging from 0 to 180 degree (for s-trans and s-cis conformations) and the corresponding values are given in Table. 2.

Considering the case of BPFTF, where its dihedral angle values are about 6.353 indicating the planar nature of the system. On the other hand, low $\langle \cos^2\phi \rangle$ values indicates that there is a higher degree of rotational disorder along the conjugated backbone in the system. Similarly, the lower $\langle \cos^2\phi \rangle$ values of the BPFTT and BPFFT indicates the smaller repulsion between the moieties in the system. Whereas in the case of BPFTF, attractive non-covalent interactions contributed to the planarity of the system. For BPTFT, the variation with respect to BP3F and BP3T is due to the increment in conjugation length leads to more resonance stabilization.

In the case of BP3F, since furan has higher aromaticity than that of thiophene moiety, its planar conformations and backbone planarization has been minimized.

Calculated frontier molecular orbitals and energy gap of the systems are given in Figure. 2. In comparison to that, pristine BP3T systems shows the HOMO value about 4.912 eV, LUMO value about 1.989 eV and the energy gap about 2.92 eV.²⁴ In all the cases, both HOMO and LUMO the electron density is distributed to the entire system. But the major localization and delocalization can be observed in thiophene and furan rings of the systems. The charge distribution over the entire system can be attributed to the high degeneracy of the molecular orbitals and it is advantageous in the case of charge mobility of the system.^{33,34}

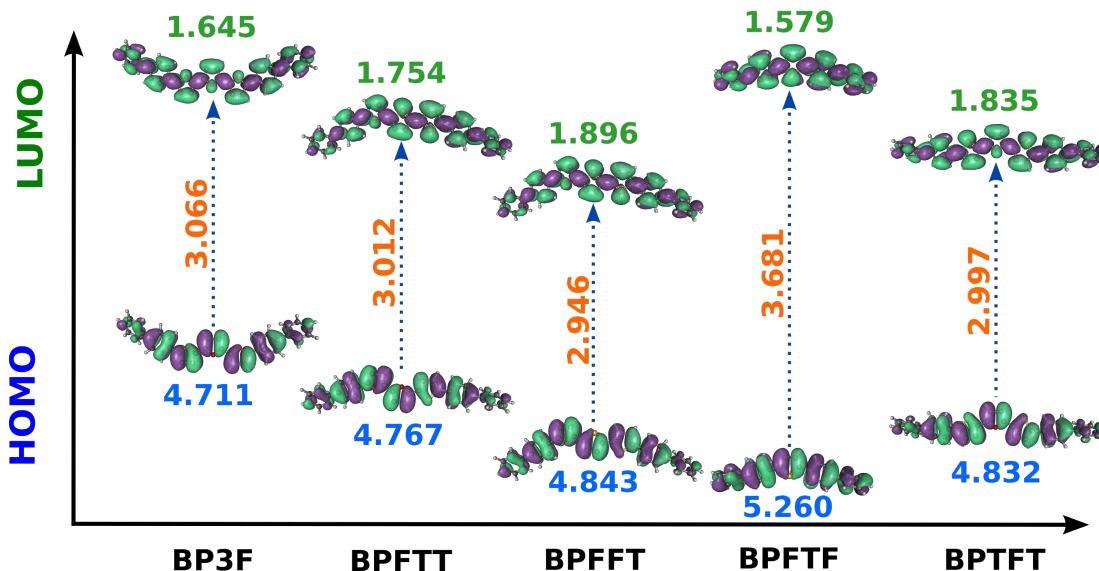


Figure 2: Electronic Properties

The band gap of the systems vary with respect to the furan substitution and BPFTF shows the maximum energy gap of 3.681 eV and BPFFT shows the minimum value about 2.946 eV. It can be seen that, higher the $\langle \cos^2\phi \rangle$ values higher the band gap values. Such a rising LUMO and lowering HOMO is a common trend expected in any conjugation system arising due to the weak bonding and antibonding on the inter ring bond.³²

Table 3: Calculated the electronic and charge transfer properties of the system

System	IP	EA	J_{eff}	λ_{hole}	λ_{elec}	μ_{hole}	μ_{elec}
BP3F	0.0045	0.0229	-0.644	8.72	0.95	5.4700	0.8830
BPFTT	0.3212	0.0620	-1.198	43.6	2.31	0.1922	0.0076
BPFFT	0.4227	0.1582	-1.325	82.8	2.75	1.8239	0.0111
BPFTF	0.2151	0.0282	-0.815	4.36	1.83	0.8892	0.0029
BPTFT	0.2173	0.0306	-1.267	4.36	0.78	2.1483	1.3156
BP3T	5.9705	1.1510	-0.016	0.10	0.96	0.8122	0.1702

Electron affinity (EA) and ionization potential (IP) values can be used to represent the oxidation and reduction capability of a molecule.^{35,36} In the present work, these values for BPFT systems were calculated using the following relations:

$$IP = E_{(cation)} - E_{(neutral)}$$

$$EA = E_{(neutral)} - E_{(anion)}$$

Here $E_{(neutral)}$, $E_{(cation)}$ and $E_{(anion)}$ are the energies of the neutral, cationic and anionic form of the each molecular system and the corresponding calculated values are given in Table. 3. Considering the OLET device architecture, the electron affinity can be interpreted to the air stability of the system and the ionization potential can be related to the hole injection.^{37,38} Often, for a p-type system lower IP values are expected.³⁹ It can be seen that with the substitution of furan rings, it would be hard to achieve the ambipolar nature in the system. Especially, BP3F shows the minimal IP values compared to the other systems with the thiophene rings. On the other hand EA values decreases with the increment of the furan rings, indicating the air stable nature of these molecules.

Computed reorganization energy (λ) values are given in Table. 3 and these values could be used to understand the charge transfer in the system by the electronic coupling between the adjacent molecules.^{40,41} In crystalline structures, these values can be used to estimate the geometry relaxations and electron-phonon coupling. λ values are inversely proportional to the mobility of the system. Thus, systems like BP3F shows higher mobility values than that of the others. For most of the systems, the hole reorganization values are one order higher than the electron reorganization energies. Further, increase in reorganization energy values are in-line with the increase of nonplanarity in the molecular systems. The charge transfer integral (CTI) values of the systems were calculated using cofacial dimers and the corresponding values are given in Table. 3. Since, planar structures are more favorable to use in an OLET device, we performed only the vertical charge transitions and excluded the tilt angle measurements. In such a case, a zero net polarization would result due to the face-to-face orientation. But due to the molecular twist results slightly distorted stacking. From the obtained values (Table. 3) it can be seen that the values increases with the incorporation of furan and the BP3F shows the highest CTI values. The reorganization energy and CTI values are used to calculate the charge transfer mobility of the system (Table.3). All the systems exhibit one order higher magnitude of hole transfer mobility than that of the electron

transfer mobility. Also, in both the cases, BPFTT shows the lowest mobility values among other furan substituted systems.

The absorption spectrum of BPFT systems are given in Fig. 3. The spectrum is similar to our previous report on BP3T system with a shoulder peak around 300 nm and the major absorption peak around 480 nm. Interestingly, in our previous study, we have observed a reasonable red shift with respect to number of thiophene rings BPT system.²⁴ But in the present study, even though slight variation in shoulder peak has been observed, the spectrum is consistent over different systems. This can be understood from the frontier molecular orbitals. Since the charge delocalization is almost same for all the systems, similar optical properties have been observed. But the slight variation in the shoulder peaks could be attributed to the planarity of the system.²⁴ Lower $\langle \cos^2\phi \rangle$ values slightly increase the absorption in the shoulder peak region. The simulated emissive spectrum is given in Fig. 4 and the corresponding oscillator strengths (f_{osc}) are given in Table. 4.

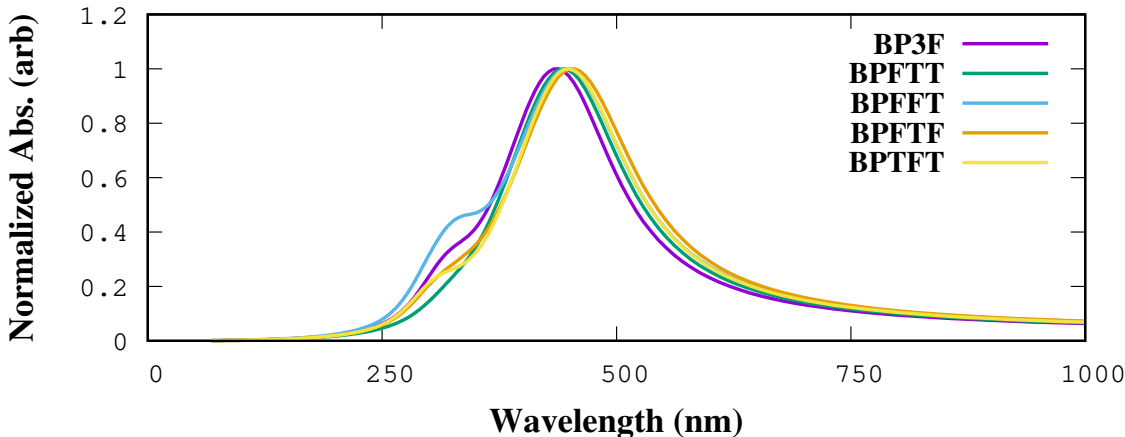


Figure 3: Absorption spectrum of pristine and furan substituted BPFT systems

The emission peaks are assigned to $\pi \rightarrow \pi^*$ transitions arising from LUMO \rightarrow HOMO transitions. In all the systems major emission is from $S_1 \rightarrow S_0$ transition and the tweaking of photoluminescence quantum yield (PLQY) can be done by modifying this transition. Using the energy gap and f_{osc} values, we have calculated the exciton binding energy values and they are in the order of BP3F $<$ BPFTT, indicating the higher exciton binding energies for

Table 4: Calculated optical parameters of pristine and furan substituted BPFT systems

System	E (cm ⁻¹)	f _{osc}	τ	TDM (au ²)
BP3F	23053.3	2.5818	1.092	36.869
BPFTT	20423.8	2.9884	1.202	48.170
BPFFT	19516.7	3.1447	1.251	53.045
BPFTF	22407.1	2.4438	1.221	35.905
BPTFT	22275.1	2.7581	1.095	40.764
BP3T	19492.0	2.3931	1.648	40.419

more than one thiophene ring substituted systems. Thus, it is easy to destroy a electron-hole pair with more number of furan rings and a higher emission is possible in these systems.

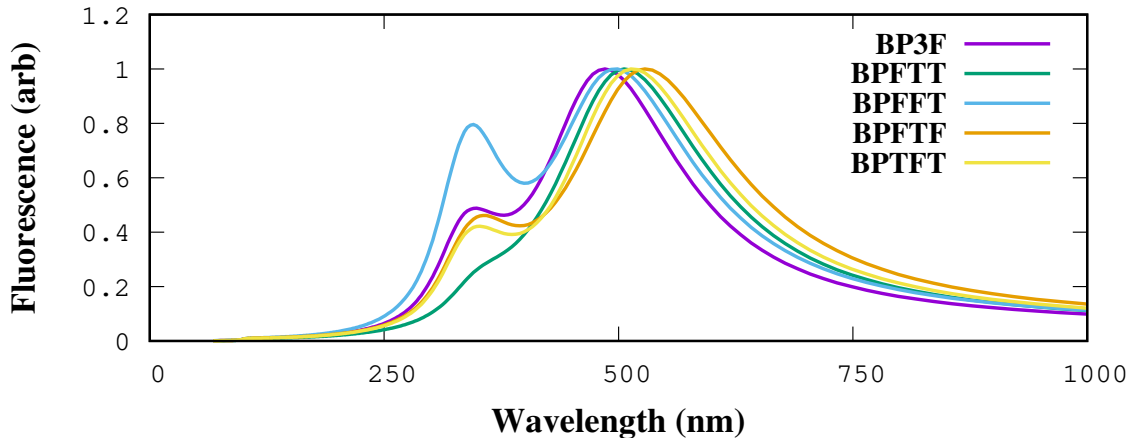


Figure 4: Emission spectrum of pristine and furan substituted BPFT systems

In optoelectronic systems, radiative lifetime values could be used to estimate the emission efficiency of the system. It can be calculated using the relation

$$\tau = \frac{1.499}{f_{osc}E^2}$$

here E is the excitation energy and the corresponding calculated values are given in Table. 4 Almost similar values indicate the strong emissive nature in all the systems. But the decrement τ values of BPFT systems with respect to pristine system can be attribute to the molecular planarity, which will be discussed in the following section. It can be further explored by using the transition dipole moment calculations (See supplementary, section 3).

Since, the maximum efficiency can be obtained with the perfect alignment of the dimers, in the present work TDM calculations were carried out along with vibrational analysis and the obtained spectrum is given in Fig. 5.^{42,43} The corresponding data can be obtained from the supplementary (Section 2). Similar to the absorption and emission spectrum the vibrational spectrum of the system is in accordance with the BP3T results. A note of warning is that, in the present case, we have considered only the molecular aspect of the furan substitution in biphenyl/thiophene system. But the experimental realization of the same material could be affected by multitude of factors ranging from crystal/thin film growth to the device fabrication and characterization methods. So, the significance of the reported data is that it could act as a potential starting point for the fabrication of prototypes and to easily explore the role of intermolecular forces in such devices.

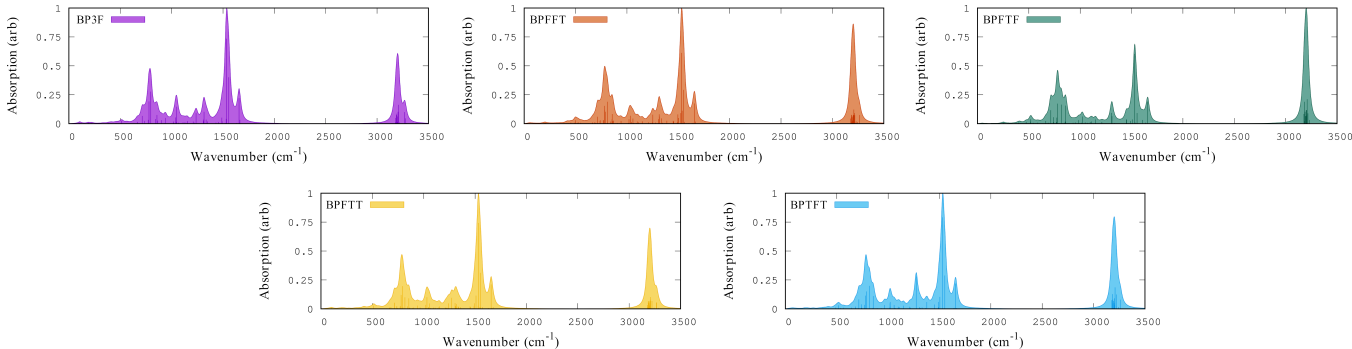


Figure 5: Vibrational frequencies and transition dipole moments of BPFT systems

Finally, in order to compare all the results, we have formulated an empirical entity (O_{eff}) which is a proportion of ratio between the product of mobilities and the $\langle \cos^2\phi \rangle$, and the product of TDM and $\langle \cos^2\phi \rangle$. This entity is derived from the fact that the ambipolar charge transfer and the transition dipole moment are related to the planarity of the molecular system and these values could be used as an estimation for the efficiency of molecular system for organic light emitting transistors. The obtained values are given in supplementary (section 4) and depicted in Fig. 6. Comparing to pristine BP3T, system with all furan, BP3F, have shown the highest O_{eff} values. This is majorly due to the higher hole transfer mobility and the lower degree of rotational disorder in the system. This was followed

by BPTFT with the value between BP3T and BP3F. In this case too, reasonable mobility with lower nonplanarity contributes to the better O_{eff} values. It is worth to note that, BPTFT is the system with highest electron mobility in the present study. These material could be better choice than BP3F, where the material’s ambipolar transport is really matters. Also, BPFTT, BPFFT and BPFTF shows lower O_{eff} values than the other three systems. In the case of BPFTF, a very strong rotational disorder highly limits these molecule for the consideration of OLETs. On the other hand, even with higher TDM values, lower values of carrier charge transport results as lower O_{eff} values for BPFTT and BPFFT systems.

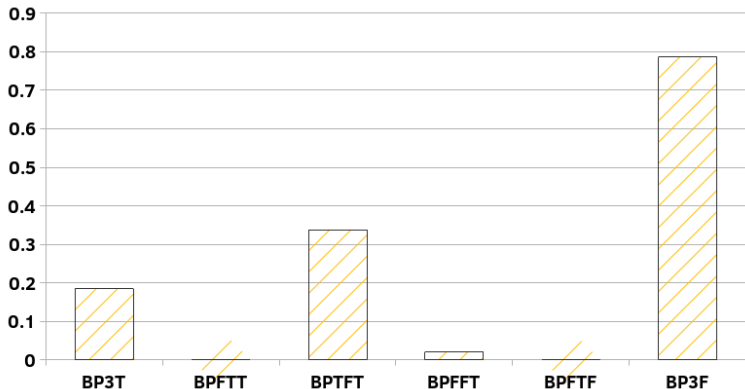


Figure 6: Comparison of all the derivatives used in the present study

4 Conclusion

The furan substituted of biphenyl/thiophenes were optimized using density functional theory with B3LYP functional and 6-311G(d,p) basis set. It is found that with the substitution of furan rings the molecular planarity significantly varies. Due to this, variation in optoelectronic properties of the system has been observed. In terms of electronic distribution, we have observed that for all the molecules the HOMO and LUMO were evenly distributed to the molecule, independent of molecular substitution. On the other hand, the substitution have altered the energy gap between HOMO and LUMO, and they are the in the range between 2.946 and 3.681. The charge transfer integral of the system are decreasing with re-

spect to the number of furan rings, where as the reorganization energy is greatly depends on the molecular planarity. With the substitution of furan the electron mobility is reduced by one fold, whereas the hole mobility is greatly improved. Considering this along with lower IP value indicates the high atmospheric stability of this material. In the case of optical properties, furan substitution does not greatly altered the absorption region of BP3T and the corresponding oscillator strengths are also similar to the pristine system. But the transition dipole moments significantly varied and the systems with either double furan or double thiophene substitution shows higher values. The radiative lifetime values decreases with the decrease in the molecular rotational disorder, i.e., more planar the molecule higher its τ values. The empirical entity O_{eff} values of BPFT systems show that BP3F has the highest value followed by BPTFT. Surprisingly, BPFTT, BPFFT and BPFTF are under performing than the pristine BP3T system, due to the higher $\langle \cos^2\phi \rangle$ values. In summary, the results confirms the potentiality of complete furan substitution in the BP3T system. But, considering the effectiveness towards OLET, selected area substitution like the BPTFT in the present case could be the optimal choice for the real life applications.

5 Supporting Information

Optimized geometries, vibrational spectra, transition dipole moments and empirical calculation details.

6 Acknowledgements

PAP and PM acknowledges the financial support from Indian Institute of Science Education and Research (IISER), Tirupati.

References

- (1) Ji, L.; Shi, J.; Wei, J.; Yu, T.; Huang, W. Air-Stable Organic Radicals: New-Generation Materials for Flexible Electronics? *Advanced Materials* **2020**, *32*, 1908015.
- (2) Dauzon, E.; Sallenave, X.; Plesse, C.; Goubard, F.; Amassian, A.; Anthopoulos, T. D. Pushing the Limits of Flexibility and Stretchability of Solar Cells: A Review. *Advanced Materials* **2021**, 2101469.
- (3) Ponnappa, S. P.; Liu, Q.; Umer, M.; MacLeod, J.; Jickson, J.; Ayoko, G.; Shid-diky, M. J.; O'Mullane, A. P.; Sonar, P. Naphthalene flanked diketopyrrolopyrrole: a new conjugated building block with hexyl or octyl alkyl side chains for electropolymerization studies and its biosensor applications. *Polymer Chemistry* **2019**, *10*, 3722–3739.
- (4) Ling, H.; Liu, S.; Zheng, Z.; Yan, F. Organic flexible electronics. *Small Methods* **2018**, *2*, 1800070.
- (5) Moser, M.; Wadsworth, A.; Gasparini, N.; McCulloch, I. Challenges to the Success of Commercial Organic Photovoltaic Products. *Advanced Energy Materials* **2021**, *11*, 2100056.
- (6) Yang, H.; Lee, J.; Cheong, J. Y.; Wang, Y.; Duan, G.; Hou, H.; Jiang, S.; Kim, I.-D. Molecular engineering of carbonyl organic electrodes for rechargeable metal-ion batteries: fundamentals, recent advances, and challenges. *Energy & Environmental Science* **2021**, *14*, 4228–4267.
- (7) Mohajeri, A.; Omidvar, A.; Setoodeh, H. Fine structural tuning of thieno [3, 2-b] pyrrole donor for designing banana-shaped semiconductors relevant to organic field effect transistors. *Journal of Chemical Information and Modeling* **2018**, *59*, 1930–1945.
- (8) Wang, Y.; Hao, W.; Huang, W.; Zhao, H.; Zhu, J.; Fang, W. Tuning the Ambipolar

- Character of Copolymers with Substituents: A Density Functional Theory Study. *The Journal of Physical Chemistry Letters* **2020**, *11*, 3928–3933.
- (9) Wang, L.; Dai, J.; Song, Y. The impact of diperfluorophenyl and thienyl substituents on the electronic structures and charge transport properties of the fused thiophene semiconductors. *International Journal of Quantum Chemistry* **2019**, *119*, e25824.
- (10) Hecht, M.; Würthner, F. Supramolecularly engineered J-aggregates based on perylene bisimide dyes. *Accounts of Chemical Research* **2020**, *54*, 642–653.
- (11) Kim, J.; Batagoda, T.; Lee, J.; Sylvinson, D.; Ding, K.; Saris, P. J.; Kaipa, U.; Oswald, I. W.; Omary, M. A.; Thompson, M. E., et al. Systematic Control of the Orientation of Organic Phosphorescent Pt Complexes in Thin Films for Increased Optical Outcoupling. *Advanced Materials* **2019**, *31*, 1900921.
- (12) Demchenko, A. P. Excitons in carbonic nanostructures. *C* **2019**, *5*, 71.
- (13) Zheng, C.; Mark, M. F.; Wiegand, T.; Diaz, S. A.; Cody, J.; Spano, F. C.; McCamant, D. W.; Collison, C. J. Measurement and theoretical interpretation of exciton diffusion as a function of intermolecular separation for squaraines targeted for bulk heterojunction solar cells. *The Journal of Physical Chemistry C* **2020**, *124*, 4032–4043.
- (14) Chaudhry, M. U.; Muhieddine, K.; Wawrzinek, R.; Sobus, J.; Tandy, K.; Lo, S.-C.; Namdas, E. B. Organic light-emitting transistors: advances and perspectives. *Advanced Functional Materials* **2020**, *30*, 1905282.
- (15) Wan, Y.; Deng, J.; Wu, W.; Zhou, J.; Niu, Q.; Li, H.; Yu, H.; Gu, C.; Ma, Y. Efficient Organic Light-Emitting Transistors Based on High-Quality Ambipolar Single Crystals. *ACS Applied Materials & Interfaces* **2020**, *12*, 43976–43983.
- (16) Ma, S.; Zhou, K.; Hu, M.; Li, Q.; Liu, Y.; Zhang, H.; Jing, J.; Dong, H.; Xu, B.; Hu, W., et al. Integrating Efficient Optical Gain in High-Mobility Organic Semiconductors for

- Multifunctional Optoelectronic Applications. *Advanced Functional Materials* **2018**, *28*, 1802454.
- (17) Dokiya, S.; Ishigami, H.; Akazawa, T.; Sasaki, F.; Yanagi, H. Organic light-emitting diodes with a PIN structure of only thiophene/phenylene co-oligomer derivatives. *Japanese Journal of Applied Physics* **2020**, *59*, 041004.
- (18) Liu, L.; Cai, C.; Zhang, Z.; Zhang, S.; Deng, J.; Yang, B.; Gu, C.; Ma, Y. Lamellar Organic Light-Emitting Crystals Exhibiting Spectral Gain and 3.6% External Quantum Efficiency in Transistors. *ACS Materials Letters* **2021**, *3*, 428–432.
- (19) Qin, Z.; Gao, H.; Dong, H.; Hu, W. Organic Light-Emitting Transistors Entering a New Development Stage. *Advanced Materials* **2021**, *33*, 2007149.
- (20) Sosorev, A. Y.; Trukhanov, V. A.; Maslennikov, D. R.; Borshchev, O. V.; Polyakov, R. A.; Skorotetcky, M. S.; Surin, N. M.; Kazantsev, M. S.; Dominskiy, D. I.; Tafeenko, V. A., et al. Fluorinated Thiophene-Phenylene Co-Oligomers for Optoelectronic Devices. *ACS Applied Materials & Interfaces* **2020**, *12*, 9507–9519.
- (21) Shang, H.; Shimotani, H.; Kanagasekaran, T.; Tanigaki, K. Separation in the Roles of Carrier Transport and Light Emission in Light-Emitting Organic Transistors with a Bilayer Configuration. *ACS Applied Materials & Interfaces* **2019**, *11*, 20200–20204.
- (22) Kanagasekaran, T.; Shimotani, H.; Shimizu, R.; Hitosugi, T.; Tanigaki, K. A new electrode design for ambipolar injection in organic semiconductors. *Nature Communications* **2017**, *8*, 1–7.
- (23) Shang, H.; Shimotani, H.; Ikeda, S.; Kanagasekaran, T.; Oniwa, K.; Jin, T.; Asao, N.; Yamamoto, Y.; Tamura, H.; Abe, K., et al. Comparative Study of Single and Dual Gain-Narrowed Emission in Thiophene/Furan/Phenylene Co-Oligomer Single Crystals. *The Journal of Physical Chemistry C* **2017**, *121*, 2364–2368.

- (24) Praveen, P. A.; Bhattacharya, A.; Kanagasekaran, T. A DFT study on the electronic and photophysical properties of biphenyl/thiophene derivatives for organic light emitting transistors. *Materials Today Communications* **2020**, *25*, 101509.
- (25) Cicoira, F.; Santato, C. Organic light emitting field effect transistors: advances and perspectives. *Advanced Functional Materials* **2007**, *17*, 3421–3434.
- (26) Turan, H. T.; Yavuz, I.; Aviyente, V. Understanding the Impact of Thiophene/Furan Substitution on Intrinsic Charge-Carrier Mobility. *The Journal of Physical Chemistry C* **2017**, *121*, 25682–25690.
- (27) Koskin, I. P.; Mostovich, E. A.; Benassi, E.; Kazantsev, M. S. Way to highly emissive materials: Increase of rigidity by introduction of a furan moiety in co-oligomers. *The Journal of Physical Chemistry C* **2017**, *121*, 23359–23369.
- (28) Zheng, B.; Huo, L. Recent Advances of Furan and Its Derivatives Based Semiconductor Materials for Organic Photovoltaics. *Small Methods* **2021**, *5*, 2100493.
- (29) Derrida, B. Velocity and diffusion constant of a periodic one-dimensional hopping model. *Journal of Statistical Physics* **1983**, *31*, 433–450.
- (30) Valeev, E. F.; Coropceanu, V.; da Silva Filho, D. A.; Salman, S.; Brédas, J.-L. Effect of electronic polarization on charge-transport parameters in molecular organic semiconductors. *Journal of the American Chemical Society* **2006**, *128*, 9882–9886.
- (31) Baumeier, B.; Kirkpatrick, J.; Andrienko, D. Density-functional based determination of intermolecular charge transfer properties for large-scale morphologies. *Physical Chemistry Chemical Physics* **2010**, *12*, 11103–11113.
- (32) Che, Y.; Perepichka, D. F. Quantifying Planarity in the Design of Organic Electronic Materials. *Angewandte Chemie International Edition* **2021**, *60*, 1364–1373.

- (33) Moliton, A.; Hiorns, R. C. Review of electronic and optical properties of semiconducting π -conjugated polymers: applications in optoelectronics. *Polymer International* **2004**, *53*, 1397–1412.
- (34) Yamaguchi, Y.; Takubo, M.; Ogawa, K.; Nakayama, K.-i.; Koganezawa, T.; Katagiri, H. Terazulene isomers: polarity change of OFETs through molecular orbital distribution contrast. *Journal of the American Chemical Society* **2016**, *138*, 11335–11343.
- (35) Ullah, H.; Ayub, K.; Ullah, Z.; Hanif, M.; Nawaz, R.; Bilal, S., et al. Theoretical insight of polypyrrole ammonia gas sensor. *Synthetic Metals* **2013**, *172*, 14–20.
- (36) Martinez, A.; Vargas, R.; Galano, A. What is important to prevent oxidative stress? A theoretical study on electron-transfer reactions between carotenoids and free radicals. *The Journal of Physical Chemistry B* **2009**, *113*, 12113–12120.
- (37) Takenobu, T.; Takano, T.; Shiraishi, M.; Murakami, Y.; Ata, M.; Kataura, H.; Achiba, Y.; Iwasa, Y. Stable and controlled amphoteric doping by encapsulation of organic molecules inside carbon nanotubes. *Nature Materials* **2003**, *2*, 683–688.
- (38) Choulis, S. A.; Choong, V.-E.; Patwardhan, A.; Mathai, M. K.; So, F. Interface Modification to Improve Hole-Injection Properties in Organic Electronic Devices. *Advanced Functional Materials* **2006**, *16*, 1075–1080.
- (39) Liu, C.-C.; Mao, S.-W.; Kuo, M.-Y. Cyanated Pentaceno[2,3-c]chalcogenophenes for Potential Application in Air-Stable Ambipolar Organic Thin-Film Transistors. *The Journal of Physical Chemistry C* **2010**, *114*, 22316–22321.
- (40) Wadsworth, A.; Chen, H.; Thorley, K. J.; Cendra, C.; Nikolka, M.; Bristow, H.; Moser, M.; Salleo, A.; Anthopoulos, T. D.; Sirringhaus, H. Modification of Indacenodithiophene-Based Polymers and its Impact on Charge Carrier Mobility in Organic Thin-Film Transistors. *Journal of the American Chemical Society* **2020**, *142*, 652–664.

- (41) Risko, C.; Kushto, G. P.; Kafati, Z. H.; Brédas, J. L. Electronic properties of silole-based organic semiconductors. *Journal of Chemical Physics* **2019**, *121*, 9031–9038.
- (42) Chuang, C.; Bennett, D. I.; Caram, J. R.; Aspuru-Guzik, A.; Bawendi, M. G.; Cao, J. Generalized kasha’s model: T-dependent spectroscopy reveals short-range structures of 2d excitonic systems. *Chem* **2019**, *5*, 3135–3150.
- (43) Yu, H.; Aziz, H. Exciton-Induced Degradation of Hole Transport Layers and Its Effect on the Efficiency and Stability of Phosphorescent Organic Light-Emitting Devices. *Advanced Optical Materials* **2019**, *7*, 1800923.

TOC Graphic

